High-T_c Superconductivity in FeSe at High Pressure: Dominant Hole Carriers and Enhanced Spin Fluctuations

J. P. Sun,[1,9] G. Z. Ye,[1,2] P. Shahi,[1] J.-Q. Yan,[3] K. Matsuura,[4] H. Kontani,[5] G. M. Zhang,[6] Q. Zhou,[2] B. C. Sales,[3] T. Shibauchi,[4] Y. Uwatoko,[7] D. J. Singh,[8,*] and J.-G. Cheng[1,†]

[1]*Beijing National Laboratory for Condensed Matter Physics and Institute of Physics, Chinese Academy of Sciences, Beijing 100190, China*

[2]*School of Physical Science and Astronomy, Yunnan University, Kunming 650091, China*

[3]*Materials Science and Technology Division, Oak Ridge National Laboratory, Oak Ridge, Tennessee 37831, USA*

[4]*Department of Advanced Materials Science, University of Tokyo, Kashiwa, Chiba 277-8561, Japan*

[5]*Department of Physics, Nagoya University, Furo-cho, Nagoya 464-8602, Japan*

[6]*State Key Laboratory of Low Dimensional Quantum Physics and Department of Physics, Tsinghua University, Beijing 100084, China*

[7]*The Institute for Solid State Physics, University of Tokyo, Kashiwa, Chiba 277-8581, Japan*

[8]*Department of Physics and Astronomy, University of Missouri, Columbia, Missouri 65211-7010, USA*

[9]*University of Chinese Academy of Sciences, Beijing 100049, China*

(Received 22 December 2016; published 7 April 2017)

The importance of electron-hole interband interactions is widely acknowledged for iron-pnictide superconductors with high transition temperatures (T_c). However, the absence of hole pockets near the Fermi level of the iron-selenide (FeSe) derived high-T_c superconductors raises a fundamental question of whether iron pnictides and chalcogenides have different pairing mechanisms. Here, we study the properties of electronic structure in the high-T_c phase induced by pressure in bulk FeSe from magnetotransport measurements and first-principles calculations. With increasing pressure, the low-T_c superconducting phase transforms into the high-T_c phase, where we find the normal-state Hall resistivity changes sign from negative to positive, demonstrating dominant hole carriers in contrast to other FeSe-derived high-T_c systems. Moreover, the Hall coefficient is enlarged and the magnetoresistance exhibits anomalous scaling behaviors, evidencing strongly enhanced interband spin fluctuations in the high-T_c phase. These results in FeSe highlight similarities with high-T_c phases of iron pnictides, constituting a step toward a unified understanding of iron-based superconductivity.

DOI: 10.1103/PhysRevLett.118.147004

The Fermi surface (FS) topology and its interplay with magnetism have been considered key ingredients in understanding the mechanism of the iron-based superconductors [1,2]. For the FeAs-based superconductors, the FS typically consists of hole- and electronlike pockets near the Brillouin zone center (Γ point) and corners (M point), respectively. As such, an interband scattering between the hole and electron pockets has been proposed as an important mechanism for electron pairing in the iron-based superconductors, leading to an $s_{\pm}$pairing state favored by the antiferromagnetic fluctuations [1,2]. This picture, however, is challenged by the observed distinct FS topology in the FeSe-derived high-T_c (>30 K) superconductors, including $A_xFe_{2-y}Se_2$ (A = K, Cs, Rb, Tl) [3], (Li,Fe)OHFeSe [4], and monolayer FeSe film [5], in which only the electron pockets are observed near the Fermi level. Thus, the distinct FS topology between FeAs- and FeSe-based materials has challenged current theories on a unified understanding of the mechanism of iron-based superconductors.

At ambient pressure, bulk FeSe is a compensated semimetal with both electron and hole FS similar to the FeAs-based materials [6–11], but without antiferromagnetism and with a low T_c [12,13]. A significant FS reconstruction takes place near the structural transition at $T_s \approx 90$ K, manifested by a dramatic splitting of d_{yz}/d_{xz} bands around both the Γ and M points [6–8]. The FS in the orthorhombic phase consists of one hole and two electron pockets with tiny carrier numbers [9]. In contrast to electron-doping approaches [14,15], the application of pressure does not introduce extra electron carriers, yet can still enhance T_c of bulk FeSe up to ∼40 K near 6 GPa [16,17]. More importantly, our recent high-pressure study has shown explicitly that the optimal T_c is achieved when the long-range antiferromagnetic order just vanishes [18], Fig. 1, reminiscent of the situations seen frequently in the FeAs-based superconductors. However, to make this connection, it is important to have information about the evolution of the FS under high pressure—a regime in which ARPES experiments are impractical, and where quantum oscillation measurements are challenging.

Here we report Hall resistivity ρ_{xy} measurements under hydrostatic pressures up to 8.8 GPa in order to gain insights into the electronic structure evolution of FeSe at high pressure. Our results demonstrate that the electrical

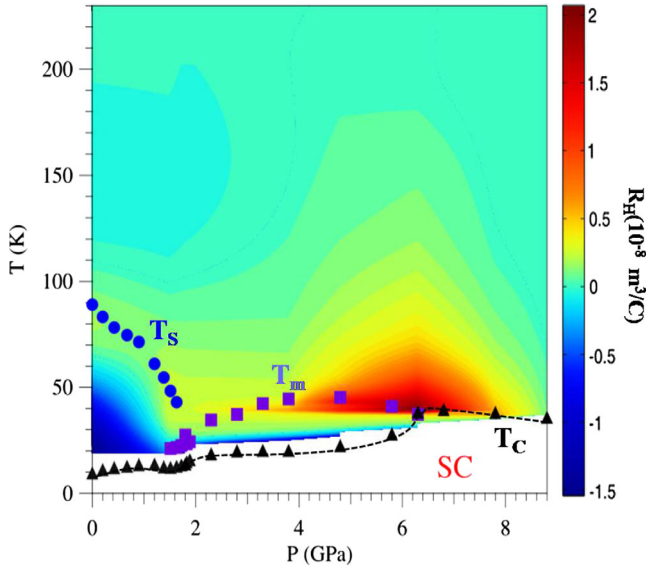

FIG. 1. Phase diagram and Hall coefficient of FeSe. Temperature-pressure phase diagram of FeSe is superimposed by a contour plot of Hall coefficient R_H, which is defined as the field derivative of ρ_{xy}, $R_H \equiv d\rho_{xy}/dH$, at the zero-field limit at each temperature and pressure. The structural (nematic) transition (T_s), pressure-induced magnetic transition (T_m), and superconducting (SC) transition (T_c) have been determined by the resistivity measurements under pressure [18]. The dashed curve is a guide for the eyes.

transport properties of FeSe at high pressures with $T_c^{\max} = 38.3$ K are dominated by the *hole* carriers, Fig. 1, which is in contrast with the known FeSe-derived high-T_c superconductors that are usually heavily electron doped. In addition, we observed an enhancement of Hall coefficient R_H near the critical pressure where the optimal T_c is realized with a simultaneous suppression of the long-range magnetic order. This implies a strong reconstruction of the Fermi surface due to antiferromagnetic (AF) order, consistent with the ordering pattern driven by interband scattering, and consistent with density functional calculations. Importantly, our results show a continuous path to high-T_c superconductivity in chalcogenides without electron doping, making a strong connection between the arsenides and chalcogenides.

Figure 2 shows the Hall resistivity $\rho_{xy}(H)$ at various temperatures under different pressures measured with the cubic anvil cell apparatus, which can maintain a relatively good hydrostaticity above 10 GPa due to the three-axis compression and the adoption of the liquid pressure transmitting medium [19]. Detailed information is given in the Supplemental Material [20]. As seen in Figs. 2(a) and 2(b), $\rho_{xy}(H)$ at 1.5 and 1.8 GPa share similar features as those at ambient pressure [10,11]. In specific, $\rho_{xy}(H)$ curves are linear for $T > 40$ K and the slope changes sign twice from positive to negative and then back to positive upon cooling, in accordance with the compensated semimetal character. A nonlinearity develops for $\rho_{xy}(H)$ below 40 K and the initial slope eventually becomes negative for $T < 30$ K, but tends

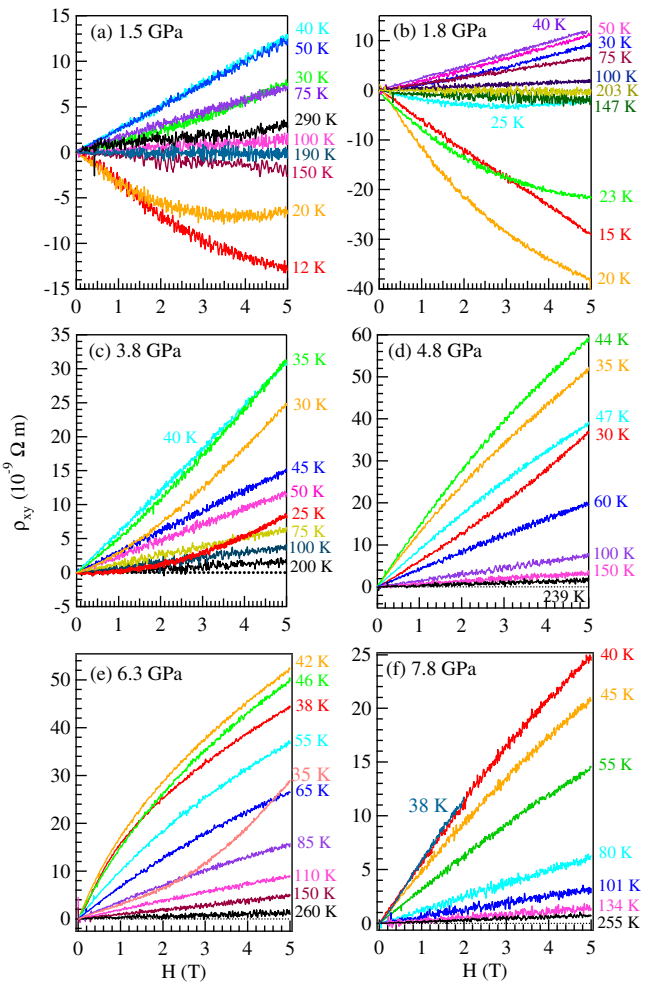

FIG. 2. Field dependence of Hall resistivity $\rho_{xy}(H)$ of a FeSe single crystal measured under various temperatures at different pressures.

to change sign again under higher magnetic field. The observation of similar low-field negative slope at ambient pressure has been ascribed to the emergence of the minority electron carriers with high mobility below T_s [10,11]. Upon increasing pressure to 3.8 GPa, surprisingly, all $\rho_{xy}(H)$ curves exhibit a positive slope without any temperature-induced sign reversal in the whole temperature range, Fig. 2(c), implying that the hole carriers become dominant. The positive slope increases gradually with decreasing temperature to 40 K, below which a nonlinearity also appears, but the initial slope remains positive down to T_c. Such a *hole* dominated Hall effect was observed to persist up to 8.8 GPa, the highest pressure in this study. As seen in Figs. 2(c)–2(f), two features are noteworthy for $3.8 \leq P \leq 8.8$ GPa. First, the linear $\rho_{xy}(H)$ at high temperatures is replaced gradually by a slightly nonlinear, concave behavior upon cooling. At 6.3 GPa, such a nonlinearity is found to persist up to 100 K. In the high-T_c cuprates, the development of such nonlinearity of $\rho_{xy}(H)$ above T_N has been attributed to the 2D AF spin fluctuations. Second,

with increasing pressure at a given temperature the $\rho_{xy}(H)$ is found to first increase and then decrease quickly. For example, ρ_{xy} at 5 T and 40 K first increases from $\sim 30 \times 10^{-9}$ Ω m at 3.8 GPa to $\sim 55 \times 10^{-9}$ Ωm at 4.8 and 6.3 GPa and then decreases to 25×10^{-9} Ωm at 7.8 GPa. As discussed below, the enhancement of ρ_{xy} correlates intimately with the AF fluctuations. Regardless of these details, the immediate message from the ρ_{xy} results is that the electronic structure of FeSe undergoes an obvious change under pressure, making the hole carriers dominating the electronic transport for $P > 3$ GPa.

To obtain the detailed information on the evolution of the Hall effect as functions of temperature and pressure, we plotted in Fig. 3 the temperature dependence of the Hall coefficient, defined as the field derivative of ρ_{xy}, $R_H \equiv d\rho_{xy}/dH$, at the zero-field limit, together with the zero-field resistivity $\rho(T)$ at each pressure. The field is applied along the c axis. As shown in Fig. 3(a), R_H at ambient pressure is small for $T > 100$ K, within the range of $\pm 0.5 \times 10^{-9}$ m^3/C, and changes sign twice upon cooling [10,11]. A moderate enhancement of R_H to $\sim 2 \times 10^{-9}$ m^3/C is evidenced towards T_s, below which R_H reverses sign again and exhibits a strong tendency to large negative values. Such a change of R_H at T_s corresponds to the FS reconstruction due to the formation of electronic nematicity [6–8], and the enhancement of R_H before T_s, if also arising from the spin fluctuations as discussed below, might support the mechanism of spin-driven nematicity [24]. As shown in Fig. 3(b), $R_H(T)$ at 1.5 GPa displays similar behaviors as that at ambient pressure, except that T_s has been shifted down to ~50 K. When the pressure is increased to 1.8 GPa, the nematic order almost vanishes and the long-range AF order starts to emerge at $T_m \approx 20$ K, which is manifested as an upturn anomaly in $\rho(T)$, Fig. 3(c). The characteristics of the nematic and AF transitions under pressure have been probed directly with the synchrotron XRD [25], μSR [26], and NMR [27] techniques recently. Although the overall behaviors of $R_H(T)$ at 1.8 GPa resemble that at 1.5 GPa, including the magnitude and the twice sign reversals for $T > 40$ K, the negative $R_H(T)$ at low temperatures exhibits a much steeper growth upon cooling below T_m with respect to those observed below T_s at 1.5 GPa. This means that a more pronounced FS reconstruction takes place at the AF order, which removes a larger portion of FS. Similar results have been reported recently by Terashima *et al.* [28,29]. Nevertheless, the major characteristics of FS topology are not expected to change up to 2 GPa given the similar Hall effects; the normal state above T_m is characterized by a compensated semimetal while that below T_m is likely dominated by the minority electron carriers with high mobility.

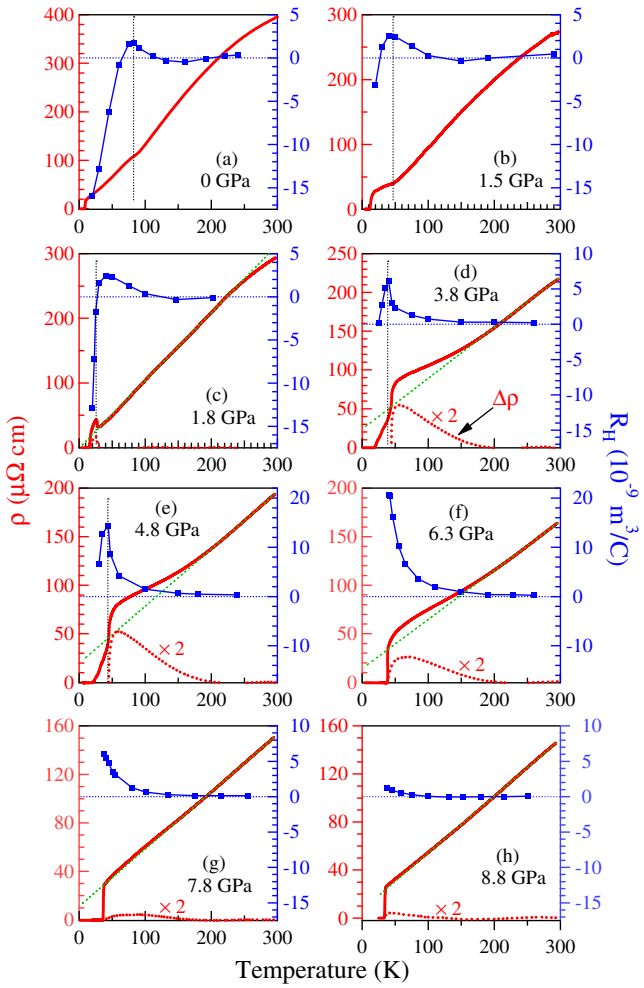

FIG. 3. Zero-field resistivity curve $\rho(T)$ (red, left axis) and the temperature dependence of the Hall coefficient R_H (blue, right axis) defined as the field derivative of ρ_{xy}, $R_H \equiv d\rho_{xy}/dH$, at the zero-field limit at each pressure. The vertical dotted lines in (a)–(e) mark the nematic order transition at T_s and the magnetic order at T_m; the horizontal dotted lines in all figures indicated the zero R_H. The resistivity difference $\Delta\rho$ (scaled by a factor of 2) was obtained by subtracting from the measured resistivity $\rho(T)$ the linear-fitting curve at high temperatures as indicated by the broken line (green).

The situation changes when the pressure is increased to above 3 GPa. As seen in Fig. 3(d) for $P = 3.8$ GPa, the AF order at $T_m \approx 40$ K is manifested as a pronounced drop in resistivity, and the positive $R_H(T)$ experiences a noticeable enhancement when approaching T_m from above. It is interesting to note that the enhancement of R_H starts around a characteristic temperature $T^* \sim 150$ K near which $\rho(T)$ exhibits a clear upward deviation from the quasi linear-in-T behavior at high temperatures. Above T^*, R_H is nearly temperature independent and takes tiny values around 0.5×10^{-9} m^3/C. Then, $R_H(T)$ decreases quickly below T_m until reaching zero around T_c. Nearly identical features are observed at 4.8 GPa, except that the enhancement at T_m becomes much stronger, Fig. 3(e); R_H at T_m increases considerably from $\sim 6 \times 10^{-9}$ m^3/C at 3.8 GPa to $\sim 14 \times 10^{-9}$ m^3/C at 4.8 GPa. Upon further increasing pressure to 6.3 GPa, the AF order becomes destabilized

and the T_c reaches the highest value of 38.3 K. As seen in Fig. 3(f), nearly T-independent R_H above $T^* \sim 150$ K is greatly enhanced upon cooling until approaching T_c; the enhancement is much more pronounced with the maximum R_H reaching $\sim 20 \times 10^{-9}$ m^3/C. Similarly, an upward deviation from the linear-T behavior of resistivity was also observed around T^*.

Upon further increasing pressure to 7.8 and 8.8 GPa, the magnetic order vanishes and T_c decreases slightly. As seen in Figs. 3(g) and 3(h), $\rho(T)$ displays a nearly perfect linear-in-T dependence in a wide temperature range from room temperature down to T_c. Concomitantly, the enhancement of $R_H(T)$ becomes much weakened and tends to diminish at 8.8 GPa, suggesting that the carrier density is greatly enhanced. These observations suggest that the enhancement of R_H correlates intimately with the deviation of resistivity from the high-temperature linear-in-T behaviors.

The major findings of the present study can be summarized in the phase diagram superimposed with the contour plot of R_H (T,P). As seen in Fig. 1, the electronic structure of FeSe in the normal state just above T_c undergoes an obvious reconstruction under pressure; it changes from the dominated electron-type to holelike around 2 GPa where the nematic order is just suppressed with a concomitant emergence of AF order. The observation of dominant hole carriers at $P > 3$ GPa, especially in the pressure range where high-T_c superconductivity can be achieved is surprising in that the hole Fermi surfaces are missing in all the known FeSe-derived high-T_c superconductors [15]. In addition, the stabilization of AF order under pressure can be attributed to the presence of hole pockets that admits FS nesting mechanisms for selecting the AF order. Although the current study puts FeSe at variance with other FeSe-derived high-T_c superconductors, the observation of high-T_c superconductivity on the border of AF order, in reminiscent of the FeAs-based superconductors, suggests that the electron-hole interband interactions are important for both FeSe under pressure and the FeAs-based superconductors.

The presence of significant AF fluctuations is supported by the enhancement of R_H above T_m centered near 6.5 GPa, Fig. 1. Since the carrier number is not expected to change considerably in the paramagnetic states, the enhancement of R_H upon cooling has to be associated with the increased scattering rate due to AF fluctuations. Indeed, the Curie-Weiss-like $R_H(T)$ has been observed in cuprate, heavy-fermion, and iron-pnictide superconductors with strong AF spin fluctuations [30,31]. In the theories involving the vertex corrections [32,33], where the backflow effect originating from the charge conservation law in the presence of strong electron correlations is taken into account [30], the enhanced R_H in the presence of AF fluctuations can be naturally understood by the enlarged AF correlation length. It has been also pointed out theoretically and observed experimentally that such strong AF fluctuations also affect the magnetoresistance $\Delta\rho_{xx}(H)/\rho_{xx}(0) = [\rho_{xx}(H) - \rho_{xx}(0)]/\rho_{xx}(0)$; unlike the conventional Kohler's rule [the scaling by $H/\rho_{xx}(0)$], the magnetoresistance can be scaled by $\tan^2\Theta_H$, where Θ_H is the Hall angle. As demonstrated in Fig. S1, the violation of Kohler's rule and the modified scaling with the Hall angle are indeed observed for our magnetoresistance data at 6.3 GPa, where the enhancement of R_H is the strongest. When the magnetic order takes place below T_m, the scattering is reduced significantly, leading to the observed resistivity drop in Figs. 3(d)–3(e).

To further understand the evolution of FS under pressure, we performed density functional calculations by using the general potential linearized augmented plane wave (LAPW) method as implemented in the WIEN2K code [34]. Details can be found in the Supplemental Material [20]. DFT calculations for FeSe are sensitive to the structure, particularly the Se position in the unit cell. We used Se positions determined from DFT calculations with AF order. This procedure gives better accord with experimental structure data than relaxation without magnetism, probably as a result of the influence of spin fluctuations on bonding in Fe-based superconductors [35]. Our DFT calculations show five sheets of FS in the nonmagnetic

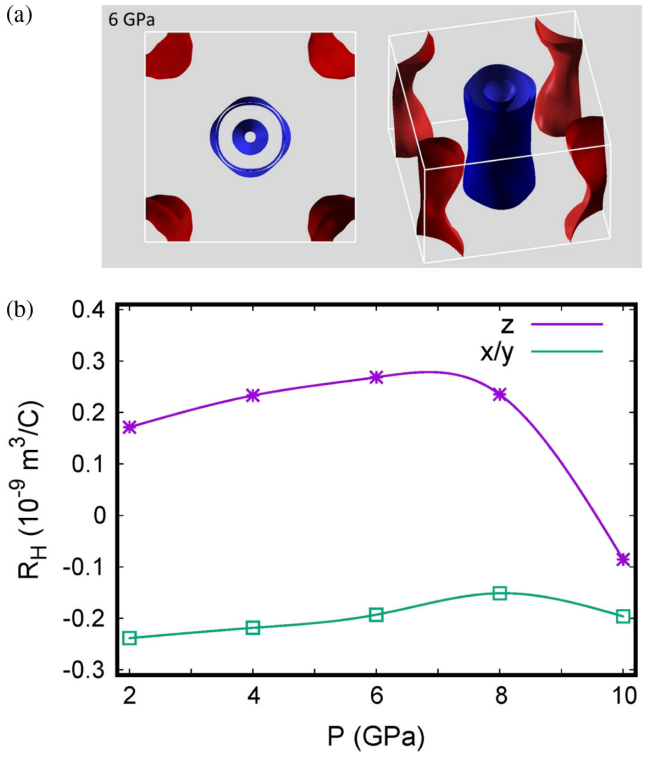

FIG. 4. (a) Results of first-principles calculations for the Fermi surface of tetragonal FeSe at 6 GPa, viewed along the c axis (left) and at an angle (right), with hole bands shown in blue and electron bands shown in red. (b) Calculated 200 K Hall coefficient as a function of pressure for field along the c axis (z, R_{xy}) corresponding to the experimental geometry, and for field in plane (x/y, R_{xz}).

tetragonal structure. The calculated FS at 6 GPa is shown in Fig. 4(a). There are three hole cylinders, containing 0.011, 0.160, and 0.191 holes per two FeSe formula unit cell, respectively, and two compensating electron cylinders with 0.209 and 0.153 electrons, respectively. The smallest hole cylinder closes off and becomes a 3D ellipsoid between 8 and 10 GPa, leading to a change in sign of the Hall number for field along the z direction. We note that the evolution of the FS with pressure up to 10 GPa is smooth, and that there are no additional surfaces, except for this closing off of the smallest hole cylinder. The DFT calculations also show an instability against the SDW-type AF order. This AF order induces the reconstruction of the FS. This reconstruction removes most of the FS, similar to results in iron pnictides [36]. This is the case both for GGA and for local spin density approximation (LSDA) calculations and in both cases the magnetic tendency is overestimated compared with experiment, qualitatively similar to the case of the FeAs-based superconductors, and presumably reflecting a large renormalization by spin fluctuations [35]. At 6 GPa the LSDA AF state has a density of states that is 0.32 of the non-spin-polarized case with a calculated moment of 1.1 μ_B/Fe.

Our constant scattering time approximation calculations based on the DFT electronic structure show a positive Hall coefficient [Fig. 4(b)] for $H//c$, consistent with experimental results, and in addition show an increase up to 6 GPa and then a decrease above 8 GPa. This tendency follows roughly the experimental observations, making a connection between the smooth evolution of the electronic structure with pressure in the DFT calculations and the experimental evolution of the Hall data. We note that these calculations do not include vertex corrections or renormalizations of the band structure that may occur, but are based only on the DFT electronic structure. This supports the conclusion that the electronic structure of FeSe remains similar to the FeAs-based superconductors with compensating zone-center hole sheets and zone-corner electron sheets including pressures where T_c is high. It is also noteworthy that the R_H is predicted to have opposite sign for the $H//ab$ plane.

In conclusion, our present high-pressure study underscores the importance of interband spin fluctuations in achieving high-T_c superconductivity in FeSe under pressure. The stabilization of AF order above 2 GPa is likely associated with the FS reconstruction with a hole-dominated character. This is consistent with a FS driven magnetic order similar to scenarios discussed for the FeAs materials. Indeed, very recent theoretical calculations [37] show that the increase of the relative Se height induces the d_{xy} hole FS pocket [one of the 3 hole pockets in Fig. 4(a)], which results in the improvements of the intra-orbital interband nesting and thus promotes the stripe-type AF order [27]. When the AF order is destabilized by the application of high pressure, the AF fluctuations may play an essential role for achieving high-T_c superconductivity as found in the FeAs-based superconductors. Thus, our present work can be considered as a significant step forward in making a unified picture on the current understanding of iron-based superconductors, specifically by demonstrating that high T_c in FeSe can be achieved with an electronic structure and other characteristics similar to the FeAs-based high-T_c superconductors.

We thank Professors Tao Xiang, Xingjiang Zhou, Jianlin Luo, Shiliang Li, and Kui Jin for very helpful discussions. This work is supported by the National Science Foundation of China (Grant No. 11574377), the National Basic Research Program of China (Grant No. 2014CB921500), the Strategic Priority Research Program and Key Research Program of Frontier Sciences of the Chinese Academy of Sciences (Grants No. XDB07020100 and No. QYZDB-SSW-SLH013). J.-Q. Y. and B. C. S.are supported by the U.S. Department of Energy, Office of Science, Basic Energy Sciences, Materials Sciences and Engineering Division. Work in Japan is supported by Grants-in-Aid for Scientific Research (KAKENHI) from Japan Society for the Promotion of Science.

J. P. S., G. Z. Y., and P. S. contributed equally to this work.

*singhdj@missouri.edu
†jgcheng@iphy.ac.cn

[1] I. I. Mazin, D. J. Singh, M. D. Johannes, and M. H. Du, Phys. Rev. Lett. **101**, 057003 (2008).
[2] F. Wang and D.-H. Lee, Science **332**, 200 (2011).
[3] T. Qian *et al.*, Phys. Rev. Lett. **106**, 187001 (2011).
[4] L. Zhao *et al.*, Nat. Commun. **7**, 10608 (2016).
[5] X. Liu *et al.*, Nat. Commun. **5**, 5047 (2014).
[6] J. Maletz *et al.*, Phys. Rev. B **89**, 220506(R) (2014).
[7] T. Shimojima *et al.*, Phys. Rev. B **90**, 121111(R) (2014).
[8] K. Nakayama, Y. Miyata, G. N. Phan, T. Sato, Y. Tanabe, T. Urata, K. Tanigaki, and T. Takahashi, Phys. Rev. Lett. **113**, 237001 (2014).
[9] T. Terashima *et al.*, Phys. Rev. B **90**, 144517 (2014).
[10] M. D. Watson *et al.*, Phys. Rev. Lett. **115**, 027006 (2015).
[11] K. K. Huynh, Y. Tanabe, T. Urata, H. Oguro, S. Heguri, K. Watanabe, and K. Tanigaki, Phys. Rev. B **90**, 144516 (2014).
[12] F.-C. Hsu *et al.*, Proc. Natl. Acad. Sci. U.S.A. **105**, 14262 (2008).
[13] T. Imai, K. Ahilan, F. L. Ning, T. M. McQueen, and R. J. Cava, Phys. Rev. Lett. **102**, 177005 (2009).
[14] B. Lei, J. H. Cui, Z. J. Xiang, C. Shang, N. Z. Wang, G. J. Ye, X. G. Luo, T. Wu, Z. Sun, and X. H. Chen, Phys. Rev. Lett. **116**, 077002 (2016).
[15] X. Liu, L. Zhao, S. He, J. He, D. Liu, D. Mou, B. Shen, Y. Hu, J. Huang, and X. J. Zhou, J. Phys. Condens. Matter **27**, 183201 (2015).
[16] S. Medvedev *et al.*, Nat. Mater. **8**, 630 (2009).
[17] H. Okabe, N. Takeshita, K. Horigane, T. Muranaka, and J. Akimitsu, Phys. Rev. B **81**, 205119 (2010).

[18] J. P. Sun *et al.*, Nat. Commun. **7**, 12146 (2016).
[19] J.-G. Cheng, K. Matsubayashi, S. Nagasaki, A. Hisada, T. Hirayama, M. Hedo, H. Kagi, and Y. Uwatoko, Rev. Sci. Instrum. **85**, 093907 (2014).
[20] See Supplemental Material http://link.aps.org/supplemental/10.1103/PhysRevLett.118.147004 for the details of high-pressure measurements and density functional calculations, the Kohler's plot of the magnetoresistance data at 6.3 GPa, as well as an alternative 3D plot of the Hall coefficient., which includes Refs. [21–23].
[21] R. S. Kumar, Yi Zhang, S. Sinogeikin, Y. Xiao, S. Kumar, P. Chow, A. L. Cornelius, and C. Chen, J. Phys. Chem. B **114**, 12597 (2010).
[22] G. K. H. Madsen and D. J. Singh, Comput. Phys. Commun. **175**, 67 (2006).
[23] L. Chaput, P. Pecheur, and H. Scherrer, Phys. Rev. B **75**, 045116 (2007).
[24] L. Fanfarillo, J. Mansart, P. Toulemonde, H. Cercellier, P. Le Fevre, F. Bertran, B. Valenzuela, L. Benfatto, and V. Brouet, Phys. Rev. B **94**, 155138 (2016).
[25] K. Kothapalli *et al.*, Nat. Commun. **7**, 12728 (2016).
[26] M. Bendele, A. Amato, K. Conder, M. Elender, H. Keller, H.-H. Klauss, H. Luetkens, E. Pomjakushina, A. Raselli, and R. Khasanov, Phys. Rev. Lett. **104**, 087003 (2010).
[27] P. S. Wang, S. S. Sun, Y. Cui, W. H. Song, T. R. Li, R. Yu, H. C. Lei, and W. Q. Yu, Phys. Rev. Lett. **117**, 237001 (2016).
[28] T. Terashima *et al.*, Phys. Rev. B **93**, 094505 (2016).
[29] T. Terashima, N. Kikugawa, S. Kasahara, T. Watashige, Y. Matsuda, T. Shibauchi, and S. Uji, Phys. Rev. B **93**, 180503 (2016).
[30] Y. Nakajima *et al.*, J. Phys. Soc. Jpn. **76**, 024703 (2007).
[31] S. Kasahara *et al.*, Phys. Rev. B **81**, 184519 (2010).
[32] S. Onari, H. Kontani, and Y. Tanaka, Phys. Rev. B **73**, 224434 (2006).
[33] L. Fanfarillo, E. Cappelluti, C. Castellani, and L. Benfatto, Phys. Rev. Lett. **109**, 096402 (2012).
[34] P. Blaha, K. Schwarz, G. K. H. Madsen, D. Kvasnicka, and J. Luitz, *WIEN2K* (Techn. Universitat Wien, Austria 2001).
[35] I. I. Mazin, M. D. Johannes, L. Boeri, K. Koepernik, and D. J. Singh, Phys. Rev. B **78**, 085104 (2008).
[36] S. E. Sebastian, J. Gillett, N. Harrison, P. H. C. Lau, D. J. Singh, C. H. Mielke, and G. G. Lonzarich, J. Phys. Condens. Matter **20**, 422203 (2008).
[37] M. Sunagawa *et al.*, J. Phys. Soc. Jpn. **85**, 073704 (2016).